



Retaining the high-temperature phases of $\text{Rb}_3\text{H}(\text{SO}_4)_2$ and $\text{Rb}_5\text{H}_3(\text{SO}_4)_4$ at room temperature

Chatr Panithipongwut KOWALSKI*

Research Unit of Advanced Materials for Energy Storage, Department of Materials Science, Faculty of Science, Chulalongkorn University, Bangkok, 10330, Thailand

*Corresponding author e-mail: chatr.p@chula.ac.th

Received date:

17 August 2021

Revised date

14 September 2021

Accepted date:

19 September 2021

Keywords:

Solid acids;
 $\text{Rb}_3\text{H}(\text{SO}_4)_2$;
 $\text{Rb}_5\text{H}_3(\text{SO}_4)_4$;
Phase transition;
Quenching

Abstract

The attempts to maintain the higher-temperature phases of $\text{Rb}_3\text{H}(\text{SO}_4)_2$ and $\text{Rb}_5\text{H}_3(\text{SO}_4)_4$ were demonstrated in this work for the first time. The goal was to explore the possibility to utilize solid acids at lower temperatures while keeping the high-temperature phases which connects to the desirable conductivities. Enabling to do so will allow the ease of handling and thermal cycling, and the energy saving in fuel cell applications, and will allow researchers to study the high-temperature properties of solid acids at lower temperatures without the expenses for the in-situ measurements and the accessibility limitations. The four relatively simple methods, which were the oven, the active airflow, the dry ice, and the liquid nitrogen methods, were selected to compare with the natural cooling at the room temperature. The dry ice and the liquid nitrogen methods for both $\text{Rb}_3\text{H}(\text{SO}_4)_2$ and $\text{Rb}_5\text{H}_3(\text{SO}_4)_4$ could not preserve the high-temperature structures at all. The other three methods worked poorly for $\text{Rb}_3\text{H}(\text{SO}_4)_2$, but quite well for $\text{Rb}_5\text{H}_3(\text{SO}_4)_4$. The oven method was the best to retain one of the $\text{Rb}_5\text{H}_3(\text{SO}_4)_4$ structures and no evidence of the original phases formed until several days later, revealing the possibility to use and study $\text{Rb}_5\text{H}_3(\text{SO}_4)_4$ at lower temperatures in the future.

1. Introduction

A solid acid, or sometimes called an acid salt, is a compound that behaves like an acid while in a solid state. This behavior refers to the proton mobility through the material which is commonly found in acids when they are dissolved in a liquid, except for a solid acid, no dissolution is required. A solid acid can be produced from a reaction between a polyprotic acid and a base, for example, H_3PO_4 or H_2SO_4 and Cs_2CO_3 or Rb_2SO_4 , with a certain ratio, specifically, the ratio must give the product containing at least one ionizable proton on the tetrahedral groups of the parent acid. A pair of an acid and a base, when mixed with different mole ratios, can yield various solid acids, for instance, $\text{Rb}_3\text{H}(\text{SO}_4)_2$ and RbHSO_4 . Common solid acids can be represented by the formula $\text{M}_p\text{H}_q(\text{XO}_4)_r$, where $\text{M} = \text{Cs}, \text{Rb}, \text{K}, \text{NH}_4$; $\text{X} = \text{S}, \text{Se}, \text{P}$; and $(p+q)/2=r$.

One of the characteristic properties of many solid acids is that their conductivities increase abruptly by 3 to 4 orders of magnitude at the temperatures where their phase transitions occur, usually $\sim 100^\circ\text{C}$ to 300°C [1-15], relatively lower than the operating temperatures of proton-conducting solid oxides. This behavior originates from the weakening of the hydrogen bonds in the crystal structure at the phase transition which allows the proton transfer from one tetrahedral group to another much faster. Thus, the transition is called the superprotonic phase transition. With this property, solid acids attract interest from many researchers aiming to use them as proton-conducting electrolytes, similar to solid oxides, in fuel cells or electrolyzers [16,17], but solid

acids can operate at lower temperatures which is beneficial in terms of thermal cycling, handling, and energy saving.

Even though $\text{Rb}_3\text{H}(\text{SO}_4)_2$ exhibits a sudden increase in conductivity like many other solid acids, the cause of the rise for this compound at 203°C is not a polymorphic phase transition, but rather a disproportionation of $\text{Rb}_3\text{H}(\text{SO}_4)_2$ to Rb_2SO_4 and the high-temperature (HT) phase of $\text{Rb}_5\text{H}_3(\text{SO}_4)_4$ — another solid acid that is already in its superprotonic phase at this temperature, hence the apparently higher conductivity [18,19]. $\text{Rb}_5\text{H}_3(\text{SO}_4)_4$, however, does not exist naturally from the room temperature all the way through 203°C . The low-temperature (LT) phase of $\text{Rb}_5\text{H}_3(\text{SO}_4)_4$ is only generated at an undetermined temperature below 140°C , but above the room temperature, from the reaction between two moles of RbHSO_4 and one mole of $\text{Rb}_3\text{H}(\text{SO}_4)_2$ [19]. After the consecutive transition at 185°C , the HT phase of $\text{Rb}_5\text{H}_3(\text{SO}_4)_4$ is formed, giving even higher conductivity, and it is the same phase that shows up in the disproportionation of $\text{Rb}_3\text{H}(\text{SO}_4)_2$. It is also noticeable that the conductivity of the LT phase is already much higher than those of the two original compounds by 2 to 3 orders of magnitude, even before the superprotonic transition. This indicates that the solid acids in this system have the possibility to be employed as the proton conductor at lower temperatures with an acceptable conductivity.

Upon cooling, some solid acids show hysteresis behaviors in the conductivity measurements [6,18-22]. The transition temperatures, determined from the sharp decrease in conductivities of these materials, are lower than those detected during the heating. This hysteresis

was also discovered even in the case of the disproportionation of $\text{Rb}_3\text{H}(\text{SO}_4)_2$ [18,19]. This nature, combined with a proper cooling process, would allow researchers to utilize solid acids at even lower temperatures.

Quenching is a known technique in which, after a heat treatment, the temperature of a sample is quickly decreased so that the material retains a specific property. Merging the concept of quenching with the hysteresis found in solid acids might help prevent phase transitions of the high-temperature phases back to the original low-temperature phases and thus, retaining the relatively high conductivities at lower temperatures.

Another benefit if the experiment is successful is that researchers can use this technique to help study HT phases of other solid acids, hopefully at room temperature, without using the in-situ measurements at elevated temperatures. The in-situ measurements, such as high-temperature X-ray diffraction (HT-XRD) measurements or high-temperature A.C. impedance spectroscopy (ACIS), are the usual methods to examine the HT phases of solid acids, but they also require specific sets of instruments or modifications of equipment to be able to carry out correctly, especially for solid acid materials that often require humidified atmosphere at high temperatures to prevent their dehydrations. These can be somewhat problematic in Thailand where the funding is limited, and the modifications of equipment usually are not allowed. The commercial equipment that can perform in-situ measurements must be imported and can be very expensive including the maintenance fees, so the number of such equipment is also few in Thailand. This is another reason why the modifications are not allowed, the price per sample is high, and the accessibility is also limited. Thus, if the outcome of the quenching is like what we hope, we can study solid acids with the regular equipment with a few additional steps, reduce the cost, and avoid the complications of the accessibility or the modifications of the in-situ equipment.

The quenching of solid acids has never been reported before and neither have the time-temperature-transformation (TTT) diagrams of any solid acids. This work will be the first attempt to explore the possibility of using quenching to maintain the high-temperature properties of solid acids and may lead to constructions of their TTT diagrams in the future. The author chose $\text{Rb}_3\text{H}(\text{SO}_4)_2$ and the $\text{Rb}_3\text{H}(\text{SO}_4)_2$ - RbHSO_4 mixture with the molar ratio of 1:2, which is the precursor for $\text{Rb}_5\text{H}_3(\text{SO}_4)_4$, to be the representatives for solid acids in this work and various simple quenching methods were investigated to serve the purposes mentioned above. The most promising method was preliminarily probed for how long it can preserve the high-temperature structure of the solid acid as well.

2. Experimental methods

2.1 Sample preparation

The $\text{Rb}_3\text{H}(\text{SO}_4)_2$ powder was prepared via organic-solvent precipitation method. Three moles of Rb_2SO_4 (99% metal basis, Alfa Aesar) and one mole of H_2SO_4 (95-97%, EMSURE) were dissolved in deionized water. The solution was then quickly poured into methanol, about 6 times by volume of the original aqueous

solution, for a complete precipitation. The precipitate was filtered and rinsed with the same solvent on a suction filter before it was placed in a drying oven at 100°C overnight.

The RbHSO_4 crystals were also obtained from an aqueous solution of Rb_2SO_4 and H_2SO_4 , but with the molar ratio of 1:2. Instead of the forced precipitation, the crystals were grown from the slow evaporation of the water. After reaching an appropriate size, > 5 mm in all dimensions, the crystals were taken out of the mother liquor, quickly rinsed with small amounts of DI water and acetone consecutively, and patted dry with kimwipes. Then the crystals were ground and left to dry in a drying oven the same as the $\text{Rb}_3\text{H}(\text{SO}_4)_2$ sample.

To prepare the precursor mixture of $\text{Rb}_5\text{H}_3(\text{SO}_4)_4$, one mole of $\text{Rb}_3\text{H}(\text{SO}_4)_2$ and two moles of RbHSO_4 were mixed and ground in a mortar for about 15 min to ensure the even distributions of the two compounds in the mixture. A desiccator with silica gel was used to store all samples prior to further examinations.

In order to smoothly handle the samples during the quenching processes and the subsequent XRD measurements, the powder samples of $\text{Rb}_3\text{H}(\text{SO}_4)_2$ and the precursor mixture of $\text{Rb}_5\text{H}_3(\text{SO}_4)_4$ were compressed into pellets. One gram of each sample was pressed using a uniaxial press to form a pellet of 12 mm diameter and 3 mm thick.

2.2 Quenching methods

To assess the effectiveness of each quenching method, the temperatures of the samples were raised up to 10°C above the temperature of the significant phase changes, specifically, 215°C for the $\text{Rb}_3\text{H}(\text{SO}_4)_2$ samples and 195°C for the $\text{Rb}_5\text{H}_3(\text{SO}_4)_4$ precursor samples. The heat treatments were carried out in a convection oven with air and the water partial pressure ($P_{\text{H}_2\text{O}}$) of about 0.02 atm to 0.03 atm for 1 h and 24 h for the $\text{Rb}_3\text{H}(\text{SO}_4)_2$ pellets and the $\text{Rb}_5\text{H}_3(\text{SO}_4)_4$ precursor pellets, respectively, to ensure the complete transformations [19,23] before the quenching steps.

As described above as one of the objectives of this work, the author chose four “quenching” methods that were relatively simple, easy to access, and cheap, to compare with leaving the samples in the room temperature to let them cool down naturally. The methods were: (1) leaving the pellet samples to cool down in the oven with the set cooling rate of $\sim 1^\circ\text{C}\cdot\text{min}^{-1}$, which gave a lower actual cooling rate of the sample temperatures, from the temperature of the heat treatment to 40°C , taking around 3.5 h, (2) using a blower to create a convection cooling at the room temperature, directing the airflow at a small angle to the surface of the pellet which was held in place by the tips of a pair of tweezers for 15 min, (3) submerging the pellets into 20 mL of acetone (slightly below 0°C) chilled with dry ice for 15 s, and (4) soaking the samples with liquid nitrogen in a small dewar for 5 s. For the convenience, these methods will be called (1) the “oven” method, (2) the “active airflow” method, (3) the “dry ice” method, and (4) the “liquid nitrogen” method, respectively. The cooling rates of the natural cooling and the four methods can be calculated to be approximately 4, 0.8, 12, 800, and $4500^\circ\text{C}\cdot\text{min}^{-1}$, respectively. It is obvious that some of the methods investigated here are not rapid cooling methods as in the definition of the term “quenching”, but for the uncomplicated references when comparing these methods, the term “quenching” is used to represent all of them.

After the results from the aforementioned methods were revealed, the oven method was chosen to survey for the length of time it can keep the high-temperature phase of $\text{Rb}_3\text{H}(\text{SO}_4)_2$. The same oven-quenched pellet of $\text{Rb}_3\text{H}(\text{SO}_4)_2$ was hastily set back to the oven at 40°C for additions of 1, 2, and 10 days, and was checked for the phase using the XRD on each of those days.

2.3 X-ray diffraction (XRD) and scanning electron microscope (SEM)

All the XRD measurements were performed using $\text{Cu K}\alpha$ radiation on a Bruker D8 Advance X-ray diffractometer. For the confirmations of the synthesized compounds, the 2θ ranged from 5 degree to 80 degree with the step size of 0.02 degree and 0.5 s per step. The XRD measurements of the pellets after the quenching were taken with the 2θ range of 15 degree to 55 degree, the 0.02-degree step size, and the time per step of 1 s, and all of the quenched samples were examined within 6 min after the quenching process. These were to assure that the handling times and the measurement times were not so long that the samples had enough time to completely transform back to the original phases, while the obtained XRD patterns still covered the range that provided enough characteristic reflections to identify the resulting phases. The electron micrographs of the samples before the heating and after the quenching were collected using JOEL JSM-6480 LV scanning electron microscope with the accelerating voltage of 5 kV to minimize the charging effect during the scan since the solid acid samples are insulating at room temperature.

3. Results and discussion

3.1 Quenching of $\text{Rb}_3\text{H}(\text{SO}_4)_2$

The XRD patterns of the $\text{Rb}_3\text{H}(\text{SO}_4)_2$ samples before the heat treatment and the natural cooling, compared with those of the samples after the four quenching methods, are shown in Figure 1(a)-(f). The reference patterns of the room-temperature (RT) phase and the HT phases of $\text{Rb}_3\text{H}(\text{SO}_4)_2$ as well as that of Rb_2SO_4 , which is a component in the HT phases of $\text{Rb}_3\text{H}(\text{SO}_4)_2$, are also shown in Figure 1(g)-(i).

The results from the samples left in the room temperature, from the oven method, and from the active airflow method in Figure 1(b), (c), and (d), respectively, exhibited the combinations of the pattern of the RT phase, major peaks at 26.6° , 30.4° , 40.9° , and 44.6° ; and the small signals from the HT pattern of $\text{Rb}_3\text{H}(\text{SO}_4)_2$, Figure 1(h), around 25.3° to 26.3° and 28.5° to 29.5° . This means that most parts in the three samples transformed back upon cooling to the original phase and only a small amount in each sample retained the high-temperature phases. In the attempt to determine the remaining amount of the HT phases, only the diffraction data of the active airflow method could be partially fit to Rb_2SO_4 , which is one of the HT phases, while the other phase could not be fit at all due to the low intensities and because of this situation, the composition percentage could not be determined.

On the other hand, the patterns of the samples quenched in the dry ice and the liquid nitrogen methods, as seen in Figure 1(e) and (f),

respectively, revealed complete reverse transitions to $\text{Rb}_3\text{H}(\text{SO}_4)_2$ as no significant peaks of the HT phases were observed at all. These findings were surprisingly unexpected since the freezing temperatures of both the dry ice in acetone and the liquid nitrogen should have provided the rapid cooling to the samples and should have been able to inhibit such transitions. So, if they were not all still in the HT phases, at least some signals from the HT phases were expected. It is still unclear what caused such outcomes, but the fact that these two methods involved liquids which exposed to the samples suggested that the liquids might play some roles in the rearrangements or the movements of the ionic groups in the crystal structure, making the phase transitions happen more easily. While there are still no reports regarding effects of the two liquids, the study by Sakashita *et al.* [24] showed that the crystalline water helped facilitate the reorientation of the tetrahedral groups in $\text{Cs}_5\text{H}_3(\text{SO}_4)_4$ and the similar effects could occur in the current work. This also brings up another possible explanation for these results, but, to the knowledge of the author, this following explanation is less likely. One could argue that because the dry ice and the liquid nitrogen are extremely cold, the water vapor in the surroundings could condense and penetrate the samples and thus, accelerated the rearrangements of the tetrahedra. However, if the condensation did occur, the amount of the water should be large enough to dissolve the solid acid samples, either partially or completely, but that was not the case during the experiments. More investigations are needed to confirm the origin of such findings.

Out of the five methods, including the natural cooling in the room temperature, the active airflow method gave the best result, yet it was unsatisfactory due to the very small amount of the high-temperature phases retained. Other quenching methods, such as chilled airflow or direct exposure to dry ice without liquids, may be studied to find the suitable way to keep the HT phases at low temperatures for $\text{Rb}_3\text{H}(\text{SO}_4)_2$.

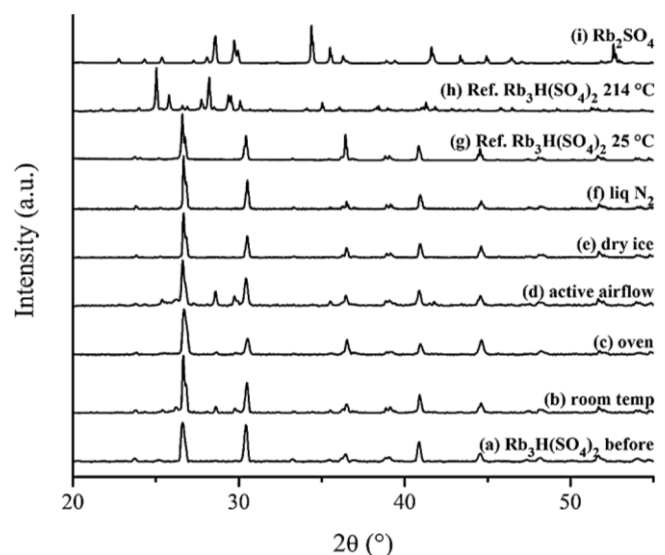


Figure 1. The XRD patterns of the $\text{Rb}_3\text{H}(\text{SO}_4)_2$ samples (a) before the heat treatment, after the quenching (b) in the room temperature, (c) via the oven method, (d) via the active airflow method, (e) via the dry ice method, and (f) via the liquid nitrogen method, compared with the published patterns of $\text{Rb}_3\text{H}(\text{SO}_4)_2$ at (g) 25°C [18] and (h) 214°C [18], and that of (i) Rb_2SO_4 .

3.2 Quenching of $\text{Rb}_5\text{H}_3(\text{SO}_4)_4$

Figure 2(a)-(f) presents the XRD patterns of the $\text{Rb}_5\text{H}_3(\text{SO}_4)_4$ precursor mixture before the heating procedure along with the five cooling approaches, respectively. The XRD patterns of $\text{Rb}_3\text{H}(\text{SO}_4)_2$ - RbHSO_4 at 25°C, LT- $\text{Rb}_5\text{H}_3(\text{SO}_4)_4$ at 160°C, and HT- $\text{Rb}_5\text{H}_3(\text{SO}_4)_4$ at 190°C are displayed in Figure 2(g)-(i) for references.

The dry ice and the liquid nitrogen methods, once again, did not deliver the desired products. None of the significant peaks of the LT and the HT phases of $\text{Rb}_5\text{H}_3(\text{SO}_4)_4$ was recognized and although their XRD patterns in Figure 2(e) and (f) were not exactly the same as either the pattern of the $\text{Rb}_3\text{H}(\text{SO}_4)_2$ - RbHSO_4 mixture (Figure 2(a)) or that of the reference (Figure 2(g)), the characteristic peaks from the two original phases already appeared at 24.0, 26.5, 30.4, 34.2, 36.4, and 40.7 degree in the sample patterns. However, the peak broadening and the different relative intensities at these positions hinted that the reverse transitions had occurred, yet still in progress. These unexpected outcomes were consistent with what were observed in the experiment of $\text{Rb}_3\text{H}(\text{SO}_4)_2$ described earlier and hence, the same theory may be used to explain what happened in this case too.

The XRD patterns of the samples from the natural cooling and the active airflow method, Figure 2(b) and (d), were practically the same and were more satisfactory as they still showed the strong signals of the key peaks of LT- $\text{Rb}_5\text{H}_3(\text{SO}_4)_4$ at 160°C, Figure 2(h), around 25.3 degree and 30.1 degree to 30.8 degree, meaning that some parts of them were still in the LT phase. Nonetheless, the peak separations and the additional small peaks at 24.0°, 26.5°, and 30.4° pointed out that the transformations back to the original phases had started, but not yet completed. The data from the active airflow could be fit to the references of all three compounds – the LT- $\text{Rb}_5\text{H}_3(\text{SO}_4)_4$, $\text{Rb}_3\text{H}(\text{SO}_4)_2$, and RbHSO_4 – giving ~35, 38, and 27 % mol, respectively, which did not agree with the molar ratio from the disproportionation reaction. This discrepancy might come from the fact that the displacement parameters of the LT- $\text{Rb}_5\text{H}_3(\text{SO}_4)_4$ phase have not been comprehensively studied and when they were applied to fit with the data at room temperature, the temperature difference could cause the error in the fitting. Another possibility is that the peak of $\text{Rb}_3\text{H}(\text{SO}_4)_2$ around 30 degree was overlapping with the peak of LT- $\text{Rb}_5\text{H}_3(\text{SO}_4)_4$ which might make the fitting incorrect. The fitting result for the natural cooling made more sense in term of $\text{Rb}_3\text{H}(\text{SO}_4)_2$ -to- RbHSO_4 ratio. The molar percentages for $\text{Rb}_5\text{H}_3(\text{SO}_4)_4$, $\text{Rb}_3\text{H}(\text{SO}_4)_2$, and RbHSO_4 were ~48, 17, and 35 % mol, respectively, giving the almost stoichiometric ratio of $\text{Rb}_3\text{H}(\text{SO}_4)_2$: RbHSO_4 of 1:2.

The oven method produced the most promising diffraction data, Figure 2(c). Though the XRD pattern of this sample did not contain the reflections from the HT- $\text{Rb}_5\text{H}_3(\text{SO}_4)_4$, Figure 2(i), it looked quite similar to the pattern of LT- $\text{Rb}_5\text{H}_3(\text{SO}_4)_4$ at 160°C in Figure 2(h), except the peak shifts, likely ascribed to the thermal expansion. Other than that, some peak broadenings and peak separations were noticeable at 25.3 degree, 30.0 degree to 31.0 degree, and around 39.5 degree to 41.8 degree, yet no signals from the major peaks of the original phases were observed, indicating that there was a rearrangement process that just started in the sample. The fact that no signals of the HT- $\text{Rb}_5\text{H}_3(\text{SO}_4)_4$ was observed was not surprising. According to the previous study by Panithipongwut *et al.* [19], the hysteresis of the reverse transition from the HT to the LT phase of $\text{Rb}_5\text{H}_3(\text{SO}_4)_4$ is small

(~10°C) and complete around 175°C, indicating that the transition can occur relatively easily, especially in the oven method where the cooling rate was below 1°C·min⁻¹, comparable to those used in the reference, so it was very likely that the HT phase would completely disappear during the cooling in this method.

A further, preliminary study on the oven method was performed to learn how long the structure of LT- $\text{Rb}_5\text{H}_3(\text{SO}_4)_4$ can be kept at 40°C. The XRD data of this sample taken after 1, 2, and 10 days in the oven are illustrated in Figure 3(c)-(e), along with those of the precursor and the sample right after cooled shown here again in Figure 3(a)-(b)

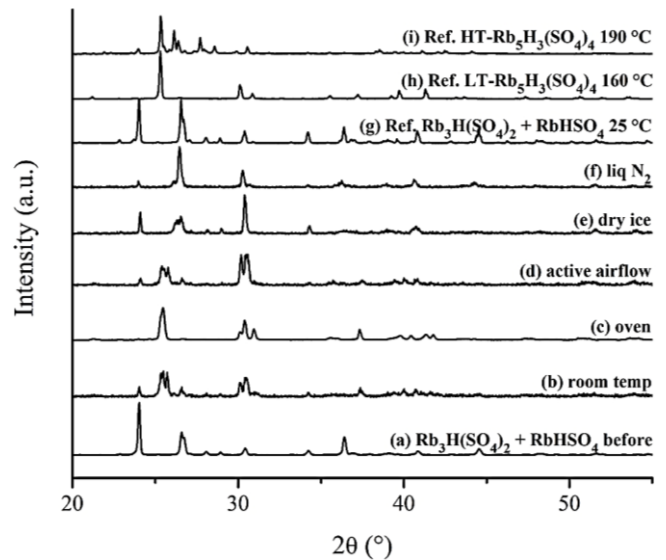


Figure 2. The XRD patterns of the $\text{Rb}_5\text{H}_3(\text{SO}_4)_4$ precursor samples (a) before the heat treatment, after the quenching (b) in the room temperature, (c) via the oven method, (d) via the active airflow method, (e) via the dry ice method, and (f) via the liquid nitrogen method, compared with the published patterns of (g) $\text{Rb}_3\text{H}(\text{SO}_4)_2$ - RbHSO_4 at 25°C [19], (h) LT- $\text{Rb}_5\text{H}_3(\text{SO}_4)_4$ at 160°C [19], and (i) HT- $\text{Rb}_5\text{H}_3(\text{SO}_4)_4$ at 190°C [19].

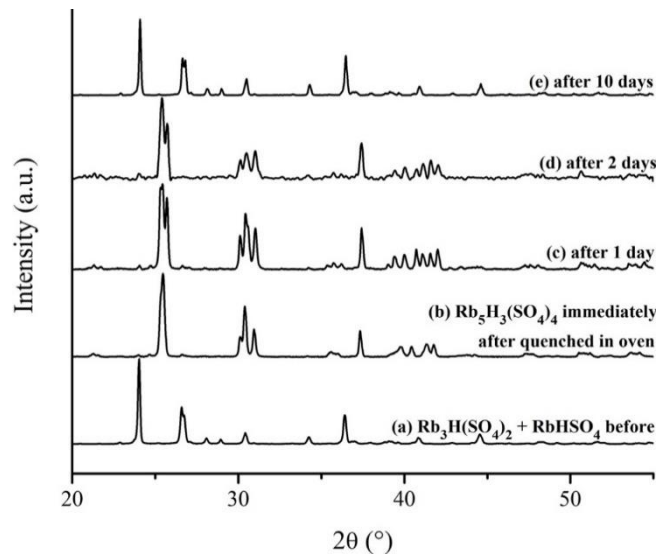


Figure 3. The XRD pattern of $\text{Rb}_5\text{H}_3(\text{SO}_4)_4$ precursor sample (a) before the heat treatment, compared with those of $\text{Rb}_5\text{H}_3(\text{SO}_4)_4$ after the quenching using the oven method (b) immediately, (c) after 1 day, (d) after 2 days, and (e) after 10 days in the oven at 40°C.

for comparison. It can be seen that after 1 day and 2 days, the phase separation occurred more as the peaks split more and started to shift slowly. Within 10 days, the sample completely transformed back to the $\text{Rb}_3\text{H}(\text{SO}_4)_2$ - RbHSO_4 mixture with the slight differences that can be seen between the patterns in Figure 3(a) and 3(e).

There are a few possible explanations why the oven method where the sample was stored at 40°C could retain the LT structure of $\text{Rb}_5\text{H}_3(\text{SO}_4)_4$ for a long time and better than preserving the HT phases of $\text{Rb}_3\text{H}(\text{SO}_4)_2$. First, the formation temperature of LT- $\text{Rb}_5\text{H}_3(\text{SO}_4)_4$ is much lower than the disproportionation temperature of $\text{Rb}_3\text{H}(\text{SO}_4)_2$ which makes the hysteresis transition of LT- $\text{Rb}_5\text{H}_3(\text{SO}_4)_4$ occur at a lower temperature, while the temperature window for the HT phases of $\text{Rb}_3\text{H}(\text{SO}_4)_2$ to transform back is much larger, from 205°C to the room temperature, thus, $\text{Rb}_3\text{H}(\text{SO}_4)_2$ has such longer time to transform that none of the chosen methods really worked. In addition, thermodynamically, the further below the transition temperature, the higher the driving force for the reverse transition. Therefore, unless the $\text{Rb}_3\text{H}(\text{SO}_4)_2$ is quenched faster, except by methods involving liquids as discussed above, it presumably will transform to the RT phase. Second, the thermodynamic aspect also leads to the possibility that the formation temperature of LT- $\text{Rb}_5\text{H}_3(\text{SO}_4)_4$ is much lower than previously estimated. The temperature range of interest was from slightly above room temperature to 140°C , leaning towards the higher end, e.g., $\sim 100^\circ\text{C}$ to 120°C , without any solid evidence. The exact temperature for the reaction of $\text{Rb}_3\text{H}(\text{SO}_4)_2$ and RbHSO_4 has never been successfully determined due to the slow kinetics of the reaction [23], but from the results in this work, the thermodynamic driving force, and the normal hysteresis sizes of 5°C to 25°C , found in previous studies of other solid acids [6,18-22], the new estimated reaction temperature could be as low as 50°C to 65°C . And if the oven temperature used in this work happened to be near the reverse transition temperature, it could simply prolong the transition time to several days as seen in the findings.

3.3 Microstructures of the quenched samples

The electron micrographs of the selected samples are depicted in Figure 4. Figure 4(a)-(c) shows the microstructures of the $\text{Rb}_3\text{H}(\text{SO}_4)_2$ powder sample before the heating, the $\text{Rb}_3\text{H}(\text{SO}_4)_2$ pellets after the oven method, and after the nitrogen method, respectively. The images did not reveal significant different among the samples, in fact including the samples of which micrographs are not shown here. The size and the shape of the particles did not change much from before the heat treatment, except some sintering effects could be seen, which was not surprising as the diffusions of the ions could happen at the high temperature. The sample of the oven method looked more connected because it was exposed to the high temperature for a much longer time than the sample quenched via the liquid nitrogen. Nevertheless, as discussed earlier from the XRD results, none of the methods gave the desired phase and the microstructures were not likely to affect nor be affected by the phase of the product.

Figure 4(d)-(f) displays the microstructures of the powder of $\text{Rb}_3\text{H}(\text{SO}_4)_2$ - RbHSO_4 mixture sample before the heating, the $\text{Rb}_5\text{H}_3(\text{SO}_4)_4$ pellets after the oven method, and after the nitrogen method, respectively. The particles in the oven method, Figure 4(e), appeared more compacted, similar to the case of the $\text{Rb}_3\text{H}(\text{SO}_4)_2$ sample.

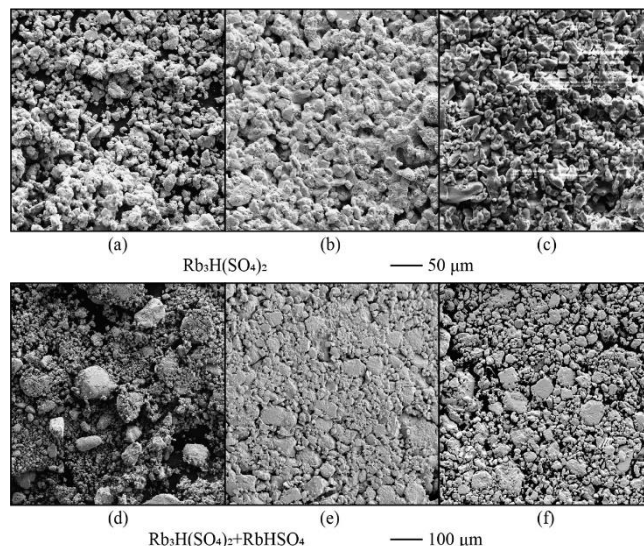


Figure 4. The electron micrographs of the $\text{Rb}_3\text{H}(\text{SO}_4)_2$ and the $\text{Rb}_5\text{H}_3(\text{SO}_4)_4$ precursor ($\text{Rb}_3\text{H}(\text{SO}_4)_2$ + RbHSO_4) samples: (a) $\text{Rb}_3\text{H}(\text{SO}_4)_2$ powder before the heat treatment, $\text{Rb}_3\text{H}(\text{SO}_4)_2$ pellets after the quenching (b) via the oven method, and (c) via the liquid nitrogen method; (d) $\text{Rb}_3\text{H}(\text{SO}_4)_2$ - RbHSO_4 powder before the heat treatment, $\text{Rb}_5\text{H}_3(\text{SO}_4)_4$ pellets after the quenching (e) via the oven method, and (f) via the liquid nitrogen method.

However, in this case, it might be related to the XRD result of this sample which indicated that the reverse reaction had not occurred for the reason as follows. $\text{Rb}_3\text{H}(\text{SO}_4)_2$ is monoclinic in the $C2/c$ space group with the lattice parameters $a=15.144(3)$ Å, $b=5.890(3)$ Å, $c=10.194(1)$ Å, and $\beta=102.55(1)^\circ$ [25], while RbHSO_4 is monoclinic in the $P2_1/c$ space group with the lattice parameters $a=14.364(8)$ Å, $b=4.623(3)$ Å, $c=14.81(1)$ Å, and $\beta=120.85(5)^\circ$ [26]. If the LT- $\text{Rb}_5\text{H}_3(\text{SO}_4)_4$ sample had transformed back to $\text{Rb}_3\text{H}(\text{SO}_4)_2$ and RbHSO_4 , the mismatch of the lattice parameters mentioned above would have forced the $\text{Rb}_5\text{H}_3(\text{SO}_4)_4$ particles to separate while the two compounds formed, like the product from the liquid nitrogen quenching in Figure 4(f), unlike the case of $\text{Rb}_3\text{H}(\text{SO}_4)_2$ where only one compound was in the product. So, in this special case, the separation of $\text{Rb}_5\text{H}_3(\text{SO}_4)_4$ back to $\text{Rb}_3\text{H}(\text{SO}_4)_2$ and RbHSO_4 might affect the micro-structure more than other solid acids, but not the other way around. Nonetheless, as long as the wanted phase is still retained and no evidence of preferred orientations was observed, the microstructure would not affect the conductivity of the solid acid.

4. Conclusions

In the comparison of the XRD patterns of the products from the natural cooling and the four selected methods, namely the oven, the active airflow, the dry ice, and the liquid nitrogen methods, for $\text{Rb}_3\text{H}(\text{SO}_4)_2$, the results were not pleasing as all of them were unable to maintain the high-temperature phases. Even the dry ice and the liquid nitrogen methods, which were anticipated to be successful, could not do so and in fact, the samples fully transformed back to the original phase. Only a few weak signals of the HT phases appeared in the patterns from the natural cooling, the oven method, and the active airflow method, indicating that most of the samples converted to the RT phase and only small parts remained in the HT phases.

For the $\text{Rb}_5\text{H}_3(\text{SO}_4)_4$ precursor samples, the same five cooling procedures were employed and three of them worked better than the case of $\text{Rb}_3\text{H}(\text{SO}_4)_2$. The dry ice and the liquid nitrogen methods still did not deliver the expected products, while the other three were able to preserve most parts of the samples in the LT- $\text{Rb}_5\text{H}_3(\text{SO}_4)_4$ phase, especially the oven method that no signals from the original phases were observed in the XRD pattern. In fact, the oven method could continue to keep the structure for at least 2 more days and more studies are needed for more specific length of time and details. The findings also suggested that the formation temperature of the LT- $\text{Rb}_5\text{H}_3(\text{SO}_4)_4$ phase was not as high as what previously thought.

The microstructures of the $\text{Rb}_3\text{H}(\text{SO}_4)_2$ samples in the various quenching method were not significantly different and seemed unrelated to the phase of the product. On the other hand, the phase separation during the cooling of $\text{Rb}_5\text{H}_3(\text{SO}_4)_4$ is likely to affect the microstructure, but not vice versa. Either way, the microstructure will not change the conductivity property of the solid acid as long as there is no preferred orientation.

The fact that the XRD result for $\text{Rb}_5\text{H}_3(\text{SO}_4)_4$ from the oven method was the best actually is beneficial as the actual fuel cell device usually runs at an elevated temperature already. Now that there is a possibility to lower the temperature and still maintain the high-temperature structure of $\text{Rb}_5\text{H}_3(\text{SO}_4)_4$, we might not have to keep the cell temperature high all the time and could reduce the energy used to operate the system and have simpler thermal cycling. Plus, it means that no additional steps of the sample preparation are necessary to study the properties of the LT phase of this solid acid, which is more convenient. The next step is to measure the conductivity of the "oven-quenched" sample whether it still gives the satisfactory conductivity for using as an electrolyte at lower temperatures and how long the conductivity can stay high before the LT phase is needed to be "re-activated" at each temperature if the sample is stored at various temperatures between the hysteresis transition temperature and the room temperature.

Acknowledgements

The author would like to thank the supporting staff at the Department of Materials Science, Faculty of Science, Chulalongkorn University for the helps with the experiments in this work. The financial support was provided by National Science and Technology Development Agency (FDA-CO-2561-8414-TH), Ministry of Higher Education, Science, Research and Innovation of Thailand.

References

- [1] E. V. Selezneva, I. P. Makarova, I. A. Malyshkina, N. D. Gavrilo, "New superprotonic crystals with dynamically disordered hydrogen bonds: Cation replacements as the alternative to temperature increase," *Acta Crystallographica Section B: Structural Science, Crystal Engineering and Materials*, vol. 73, no. Pt 6, pp. 1105-1113, 2017.
- [2] D. Z. Yi, S. Sanghvi, C. P. Kowalski, and S. M. Haile, "Phase behavior and superionic transport characteristics of $(\text{M}_x\text{Rb}_{1-x})_3\text{H}(\text{SeO}_4)_2$ ($\text{M} = \text{K}$ or Cs) solid solutions," *Chemistry and Materials*, vol. 31, no. 23, pp. 9807-9818, 2019.
- [3] A. Ikeda, D. A. Kitchaev, and S. M. Haile, "Phase behavior and superprotonic conductivity in the $\text{Cs}_{1-x}\text{Rb}_x\text{H}_2\text{PO}_4$ and $\text{Cs}_{1-x}\text{K}_x\text{H}_2\text{PO}_4$ systems," *Journal of Materials Chemistry A*, vol. 2, no. 1, pp. 204-214, 2014.
- [4] A. Ikeda, and S. M. Haile, "Examination of the superprotonic transition and dehydration behavior of $\text{Cs}_{0.75}\text{Rb}_{0.25}\text{H}_2\text{PO}_4$ by thermogravimetric and differential thermal analyses," *Solid State Ionics*, vol. 181, no. 3-4, pp. 193-196, 2010.
- [5] Y. K. Taninouchi, T. Uda, Y. Awakura, A. Ikeda, and S. M. Haile, "Dehydration behavior of the superprotonic conductor CsH_2PO_4 at moderate temperatures: 230 to 260 degrees C," *Journal of Materials Chemistry*, Article vol. 17, no. 30, pp. 3182-3189, 2007.
- [6] S. M. Haile, C. R. I. Chisholm, K. Sasaki, D. A. Boysen, and T. Uda, "Solid acid proton conductors: from laboratory curiosities to fuel cell electrolytes," *Faraday Discussions*, vol. 134, pp. 17-39, 2007.
- [7] S. Takeya, S. Hayashi, H. Fujihisa, and K. Honda, "Phase transition in a superprotonic conductor $\text{Cs}_2(\text{HSO}_4)(\text{H}_2\text{PO}_4)$ induced by water vapor," *Solid State Ionics*, vol. 177, no. 15-16, pp. 1275-1279, 2006.
- [8] Y. Matsuo, J. Hatori, Y. Yoshida, K. Saito, and S. Ikehata, "Proton conductivity and spontaneous strain below superprotonic phase transition in $\text{Rb}_3\text{H}(\text{SeO}_4)_2$," *Solid State Ionics*, vol. 176, no. 31-34, pp. 2461-2465, 2005.
- [9] Y. Matsuo, Y. Tanaka, J. Hatori, and S. Ikehata, "Proton activity and spontaneous strain of $\text{Cs}_3\text{H}(\text{SeO}_4)_2$ in the phase transition at 369 K," *Solid State Communications*, vol. 134, no. 5, pp. 361-365, 2005.
- [10] S. M. Haile, K. D. Kreuer, and J. Maier, "Structure of $\text{Cs}_3(\text{HSO}_4)_2(\text{H}_2\text{PO}_4)$ - a new compound with a superprotonic phase transition," *Acta Crystallographica Section B-Structural Science*, vol. 51, pp. 680-687, 1995.
- [11] S. M. Haile, G. Lentz, K. D. Kreuer, and J. Maier, "Superprotonic Conductivity in $\text{Cs}_3(\text{HSO}_4)_2(\text{H}_2\text{PO}_4)$," *Solid State Ionics*, vol. 77, pp. 128-134, 1995.
- [12] S. M. Haile, P. M. Calkins, and D. Boysen, "Superprotonic conductivity in beta- $\text{Cs}_3(\text{HSO}_4)_2(\text{H}_x(\text{P,S})\text{O}_4)$," *Solid State Ionics*, vol. 97, no. 1-4, pp. 145-151, 1997.
- [13] C. R. I. Chisholm, and S. M. Haile, "Structure and thermal behavior of the new superprotonic conductor $\text{Cs}_2(\text{HSO}_4)(\text{H}_2\text{PO}_4)$," *Acta Crystallographica Section B-Structural Science*, vol. 55, pp. 937-946, 1999.
- [14] C. R. I. Chisholm, and S. M. Haile, "Superprotonic behavior of $\text{Cs}_2(\text{HSO}_4)(\text{H}_2\text{PO}_4)$ - a new solid acid in the CsHSO_4 - CsH_2PO_4 system," *Solid State Ionics*, vol. 136, pp. 229-241, 2000.
- [15] O. S. Hernández-Daguer, H. Correa, and R. A. Vargas, "Phase behaviour and superionic phase transition in $\text{K}_3\text{H}(\text{SeO}_4)_2$," *Ionics*, vol. 21, no. 8, pp. 2201-2209, 2015.
- [16] D.-K. Lim, J. Liu, S. A. Pandey, H. Paik, C. R. I. Chisholm, J. T. Hupp, and S. M. Haile, "Atomic layer deposition of $\text{Pt}@ \text{CsH}_2\text{PO}_4$ for the cathodes of solid acid fuel cells," *Electrochimica Acta*, vol. 288, pp. 12-19, 2018.

- [17] D.-K. Lim, A. B. Plymill, H. Paik, X. Qian, S. Zecevic, C. R. I. Chisholm, and S. M. Haile, "Solid Acid Electrochemical Cell for the Production of Hydrogen from Ammonia," *Joule*, vol. 4, no. 11, pp. 2338-2347, 2020.
- [18] L. A. Cowan, R. M. Morcos, N. Hatada, A. Navrotsky, and S. M. Haile, "High temperature properties of $\text{Rb}_3\text{H}(\text{SO}_4)_2$ at ambient pressure: Absence of a polymorphic, superprotonic transition," *Solid State Ionics*, vol. 179, no. 9-10, pp. 305-313, 2008.
- [19] C. Panithipongwut, and S. M. Haile, "High-temperature phase behavior in the $\text{Rb}_3\text{H}(\text{SO}_4)_2$ - RbHSO_4 pseudo-binary system and the new compound $\text{Rb}_5\text{H}_3(\text{SO}_4)_4$," *Solid State Ionics*, Article; Proceedings Paper vol. 213, pp. 53-57, 2012.
- [20] A. I. Baranov, "Crystals with disordered hydrogen-bond networks and superprotonic conductivity. Review," *Crystallography Reports*, vol. 48, no. 6, pp. 1012-1037, 2003.
- [21] M. W. Louie, M. Kislitsyn, K. Bhattacharya, and S. M. Haile, "Phase transformation and hysteresis behavior in $\text{Cs}_{1-x}\text{Rb}_x\text{H}_2\text{PO}_4$," *Solid State Ionics*, vol. 181, no. 3-4, pp. 173-179, 2010.
- [22] A. Pawlowski, L. Szczesniak, M. Polomska, B. Hilczer, and L. Kirpichnikova, "Pretransitional effects at the superionic phase transition of $\text{Rb}_3\text{H}(\text{SeO}_4)_2$ protonic conductor," *Solid State Ionics*, vol. 157, no. 1-4, pp. 203-208, 2003.
- [23] C. P. Kowalski, P. Chaijaroen, and F. Kaewniyom, "Thermal behavior of solid acids in the $\text{Rb}_3\text{H}(\text{SO}_4)_2$ - RbHSO_4 system under ambient atmosphere," *Journal of Metals, Materials and Minerals*, vol. 31, no. 1, pp. 57-63, 2021.
- [24] M. Sakashita, H. Fujihisa, K. I. Suzuki, S. Hayashi, and K. Honda, "Using X-ray diffraction to study thermal phase transitions in $\text{Cs}_5\text{H}_3(\text{SO}_4)_4 \cdot x\text{H}_2\text{O}$," *Solid State Ionics*, vol. 178, no. 21-22, pp. 1262-1267, 2007.
- [25] S. Fortier, M. E. Fraser, and R. D. Heyding, "Structure of trirubidium hydrogenbis(sulfate), $\text{Rb}_3\text{H}(\text{SO}_4)_2$," *Acta Crystallographica Section C*, vol. 41, no. 8, pp. 1139-1141, 1985.
- [26] K. Itoh, H. Ohno, and S. Kuragaki, "Disordered structure of ferroelectric rubidium hydrogen sulfate in the paraelectric phase," *Journal of the Physical Society Japan*, vol. 64, no. 2, pp. 479-484, 1995.